Proceedings of ICFDP8
Eighth International Congress of Fluid Dynamics & Propulsion
December 14-17, 2006, Sharm El-Shiekh, Sinai, Egypt

ICFDP8-EG-131

EXPERIMENTAL AND NUMERICAL STUDY OF THE EFFECT OF TIP CLEARANCE ON THREE-DIMENSIONAL FLOW FIELD THROUGH LINEAR TURBINE CASCADE

H. El-Batsh **
Mechanical Engineering Technology Department,
Benha High Institute of Technology,
Benha University, Benha, Egypt

M. Bassily Hanna, M. F. Sherif
Mechanical Power Engineering and Energy Department, Faculty of Engineering,
Minia University, Minia, Egypt

ABSTRACT

Profile loss, secondary flow loss and tip leakage flow are the main causes of turbine blade losses. The flow in the tip region with tip clearance is quite complex. The interaction of the leakage flow, secondary flow and the boundary layer flow around the blade introduce a three-dimensional complex flow structure. In addition, the relative motion between the blade and the casing makes the flow more complex. This study aims to improve the understanding of the three dimensional flow field within turbine blade passage and in the tip clearance region. The paper aims also to investigate the effect of the tip clearance gap on the flow field and on loss mechanism in turbine blades using experimental measurements as well as CFD numerical calculations. The flow measurements are obtained using a set of calibrated five-hole pressure probes. The turbulent flow field is calculated by using a recent one-equation model namely Spalart-Allmaras model. The total pressure loss coefficient is estimated downstream of the cascade.

1. INTRODUCTION

The applications of gas turbines are growing in all fields of applications. Therefore, a detailed and fundamental comprehension of loss mechanisms in gas turbines is necessary. Profile loss, secondary flow loss and tip leakage flow are the main causes of turbine blade losses. Investigation for the profile loss at design and off design conditions was performed by El-Batsh [1]. Sieverding [2] gave an overview for different types of secondary flows in turbine blades and their effect on loss mechanism. El-Batsh and Bassily Hanna [3] performed three-dimensional calculations for the flow inside turbine blade passages and estimated the secondary flow loss.

Clearance gaps between the rotating blades and the casing exist in all gas turbine engines. In an unshrouded turbine stage, this gap is typically of the order 1% blade height and changes during operation due to thermal expansion. The leakage flow through tip clearance gap is caused by the pressure difference between the pressure and suction surfaces of the blade. The tip leakage flow causes significant reduction in the aerodynamic performance of the stage. Losses occur as the leakage flow interacts with the passage flow and form viscous forces acting within the tip gap itself. Furthermore there is a reduction in work output from the rotor as the leakage flow is unturned. Denton [4] noted that the flow through the tip gap between the unshrouded rotor blades and the casing is responsible for high losses in axial flow gas turbines. As a consequence, the designer of gas turbine engines is interested in the proper understanding of the various features of the tip leakage flow. Moore and Tilton [5] investigated the tip clearance flow in a linear turbine cascade. They measured flow velocities in the gap between casing and blade tip using pressure taps at the top of the profile. Bindon [6] determined the internal gap loss along the chord for several tip clearance gap sizes in a cascade. Most experimental studies on tip leakage flow were performed stationary. Very few experimental studies considered the effect of the relative motion between the blades and end-wall. Yaras and Sjolander [7] and Yaras et al. [8] simulated the relative motion by using a moving belt at the end-wall. Willinger and Haselbacher [9,10] performed CFD calculations for the flow in turbine blade passages including the effect of the tip clearance. They did not

** Correspondence author
Tel: +20-10-2036287, Email: helbatsh@yahoo.com

consider the effect of the relative movement between the blades and the wall. The effect of blade geometry at the tip region on the tip leakage flow was investigated by Krishnababu et al. [11].

The mechanical power engineering and energy department of Minia University, Egypt started cooperation program with the mechanical engineering technology department of Benha High Institute of Technology, Benha University, Egypt. The program aims to improve the understanding of the three-dimensional flow field within turbine blade passages and in the tip clearance region. For this purpose, an experimental set-up is built to obtain detailed experimental measurements. The experimental set-up allows the measurement in the tip clearance gap when the end-wall is moving in order to simulate the real machine. CFD calculations are also performed to investigate the flow. The data presented in this paper represent the first part of the study which includes the description of the experimental technique and the CFD calculations. Four different values for the tip clearance gaps k are examined. These values are 1%, 2.4%, 4.8% and 10% of the blade height h. While the 1% value is a typical value used in gas turbines, larger values are considered as well because they are useful for experimental verification and they make the loss mechanism more understandable. In order to determine the tip leakage loss, the losses for the same cascade without tip clearance are estimated. The tip clearance loss is the difference between the total losses for the cases with tip clearance minus the losses without the tip clearance.

2. EXPERIMENTAL PROCEDURE

2.1 Experimental set-up

A low speed wind tunnel exhausting to the atmosphere is used in this study to obtain the experimental measurements. The cascade test section (Fig. 1) includes five blades with a profile similar to that used by Langstone et al. [12]. The cascade parameters are given in table 1.

Table 1: cascade parameters

Chord, c [mm]	168
Axial chord, c_x [mm]	144
Blade spacing , s [mm]	170
Blade inlet angle, β_1 [°]	40
Blade exit angle, β_2 [°]	65
Stagger angle, γ [°]	35
Incidence angle, i [°]	0
Blade height, h [mm]	124.5
Aspect ratio, [–]	0.74
Tip clearance/blade height, k/h [%]	1, 2.4, 4.8, 10

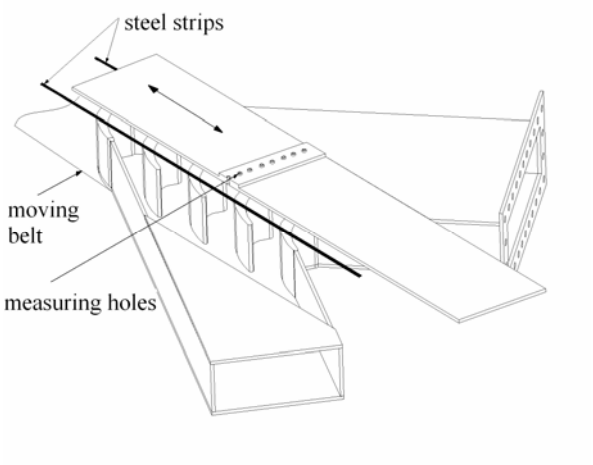

Figure 1: Experimental test section

The blades are mounted from the upper-end to the test section which represents the stationary side. In order to simulate the movement of the blades while the test section is fixed, a moving belt is used at the lower-end side (Fig. 1). The normal distance between the belt and the tip of the blades represents the tip clearance gap. The tip clearance gap could be changed to investigate its effect on the flow field. The speed of the belt could also be changed. Measurements are obtained using calibrated five-hole pressure probe inserted from the top through predefined holes. The location of the holes relative to the blades is changed to allow the measurements at different planes through the blade channel. This is achieved by fixing the blades from their upper-end in two steel strips. These strips are allowed to slide in two ways on the upper-end wall (Fig.1).

The flow field is measured using a set of calibrated five-hole probes. The diameter of the probe head is 3 mm. The calibration is performed by placing the probes in free jet where the velocity is uniform and constant. Effect of probe orientation on the measured pressures is represented by dimensionless pressure coefficients. Calibrations curves are obtained representing the relation between probe angles and pressure coefficients. The range of the calibration angle is ±30 degrees. All pressure measurements are obtained by using a digital micro-manometer with accuracy of 0.1 mm. The inlet flow conditions are measured at the axial position of 0.64 c_x from the blade leading edge. The wake distribution is measured at two planes downstream of the cascade at distances of $1.11\,c_x$ and $1.32\,c_x$.

2.2 Measurement Uncertainty

Probes are usually calibrated in a well-controlled calibration tunnel. They are used to measure the flow through turbine blade passages in which the Reynolds number, Mach number, and turbulence intensity are different from the corresponding values during

calibration. The measurement error when the five-hole probe is used in turbomachinery is mainly caused by the effects of Reynolds number, compressibility, turbulence, velocity gradients, probe-wall distance and probe blockage. An extensive review was performed by Sevilla [13] for the effect of these parameters on the accuracy of measurements obtained by five-hole probes. Sevilla found that the increase in Reynolds number by an order 2.3 produces a maximum error of 2.8% in velocity measurements. It was also noted that the error caused by neglecting the effect of compressibility is about 1% when the Mach number is 0.28. The review of Sevilla revealed that the percentage error in the stagnation pressure measurement is about 0.5 times turbulence intensity. When the probe is adjacent to a wall, the error is negligible when the distance between the probe and the wall is more than two probe diameters. Finally, in the present study, the blockage ratio is very small and could be neglected.

3. NUMERICAL PROCEDURE

In the numerical procedure, the flow field is obtained by solving the governing equations for the steady incompressible isothermal flow. The flow is solved in a single flow channel. Since the flow is repeated in different channels, periodic boundary conditions are used. The inlet plane is chosen as a distance of 0.64 c_x upstream of the cascade and the exit boundary is considered at a distance of 1.76 c_x downstream of the cascade.

3.1 Governing Equations

The turbulent flow is calculated by solving the Reynolds Averaged Navier-Stokes (RANS) equations. For steady incompressible flow, RANS equations can be written in Cartesian coordinates as:

$$\frac{\partial u_j}{\partial x_j} = 0 \tag{1}$$

$$\frac{\partial \left(u_i u_j\right)}{\partial x_j} = -\frac{1}{\rho}\frac{\partial P}{\partial x_i} + \frac{1}{\rho}\frac{\partial \left(\tau_{ij}\right)}{\partial x_j} \tag{2}$$

u_i and u_j are the velocities in i and j directions, P is the pressure and ρ is the density. The effective stress tensor τ_{ij} in the above mean equations is given by:

$$\tau_{ij} = \mu_{\text{eff}}\left[\frac{\partial u_i}{\partial x_j} + \frac{\partial u_j}{\partial x_i}\right] - \frac{2}{3}\mu_{\text{eff}}\left[\frac{\partial u_k}{\partial x_k}\right]\delta_{ij} \tag{3}$$

The effective viscosity μ_{eff} is represented by the summation of laminar viscosity μ and turbulent viscosity μ_t using eddy-viscosity based model:

$$\mu_{\text{eff}} = \mu + \mu_t \tag{4}$$

Spalart and Allmaras [14] proposed a relatively simple one-equation model that solves a single transport equation for the turbulent kinematic viscosity $\tilde{\nu}$. The turbulent viscosity is computed as:

$$\mu_t = \rho \tilde{\nu} f_{\nu 1} \tag{5}$$

The viscous damping function $f_{\nu 1}$ is given by:

$$f_{\nu 1} = \frac{X}{X^3 + C_{\nu 1}^3} \tag{6}$$

$$X \equiv \frac{\tilde{\nu}}{\nu} \tag{7}$$

where $C_{\nu 1}$ is a constant and ν is the molecular kinematic viscosity.

The transport equation for $\tilde{\nu}$ in the Spalart-Allmaras model is

$$\frac{\partial}{\partial x_i}\left(\rho \tilde{\nu} u_i\right) = G_\nu + \frac{1}{\sigma_{\tilde{\nu}}}\left[\frac{\partial}{\partial x_j}\left(\left(\mu + \rho\tilde{\nu}\right)\frac{\partial \tilde{\nu}}{\partial x_j}\right) + C_{b2}\rho\left(\frac{\partial \tilde{\nu}}{\partial x_j}\right)^2\right] - Y_\nu \tag{8}$$

where G_ν is the production of turbulent viscosity and Y_ν is the destruction of turbulent viscosity, that occurs in the near-wall region due to wall blocking and viscous damping. $\sigma_{\tilde{\nu}}$ and C_{b2} are constants.

The model constants have the following values:
$\sigma_{\tilde{\nu}} = 2/3$, $C_{b2} = 0.622$, $C_{\nu 1} = 7.1$

3.2 Computational Grid

Four different computational grids are generated for different values of tip clearance gap. The grid is generated for the total blade height and the tip clearance gap. The computational grids have about 535,000 grid points (Fig. 2). The calculations using grids with this large number of cells require large computer resources with high speed and large memory and it requires long computational time. The personal computer used to perform these calculations has 1 GB Ram and Pentium 4 processor with 1.7MHz frequency. Using grids with these numbers of grid points reach the maximum possible number of grid points allowed for the used computer. Therefore, checking the grid-dependency on the results by increasing the number of grid points could not be performed here.

Hildebrandt and Fottner [15] studied the effect of grid refinement on the flow field inside a highly loaded turbine cascade. They found that the grid independent solution could be obtained with a total number of grid points of about 300,000 when the half blade span is

modeled. The blade aspect ratio of the blade which they had used is 3 while the blade used in the present study has the aspect ratio of 0.74. Therefore, the blade used here is shorter than the blades used by Hildebrandt and Fottner and requires less grid points. Based on their results, the solutions obtained in the present study are grid-independent.

The computational domain is divided into six blocks and the grid is generated in each block individually. Two blocks exist in the flow channel as shown in Fig. 2b and four blocks exist in the tip clearance gap (Fig. 2c). This method of grid generation allows the possibility of generating dense grid near the walls and coarse grid far from the walls and therefore, better distribution of the grid points as shown in Fig. 2. The grid is characterized by an O-grid shape near to the blade and H-grid in the remainder domain. The O-grid near the blade allows the accurate solution of the blade boundary layer. The grid is unstructured in the blade cross section and is structured in the direction of the blade height. Careful attention has been paid to minimize for the grid skewness and cell aspect ratio that are required to obtain faster convergence and accurate results.

3.3 Boundary Conditions

At the inlet boundary, the velocity profile, turbulence intensity and eddy length scale are defined. The inlet boundary layer thickness affects the intensity of secondary flow and tip leakage. Therefore, the velocity distribution at the inlet is obtained from the experimental measurements and is used at the inlet boundary. Turbulence intensity and length scale are not measured here. Casey and Wintergerste [16] introduced guidelines for the specification of turbulence quantities at the inlet. Turbulence intensity and length scale are assumed in the present study based on these guidelines. Turbulence intensity is considered here as 5% and the inlet characteristic length is assumed as 0.07 of the hydraulic diameter at the inlet. The calculations are performed here with stationary end-wall.

3.4 Solution Procedure

A control-volume-based technique is used to convert the differential equations to algebraic equations which can be solved numerically. The convection terms of the governing equations is achieved by using the Quadratic Upwind Interpolation Scheme (QUICK).

The Semi-Implicit Method for Pressure-Linked Equations (SIMPLE) as developed by Patanker [17] is used to solve the discretized equations. The equations are solved in iterations and the solution loop is repeated until a converged solution is obtained

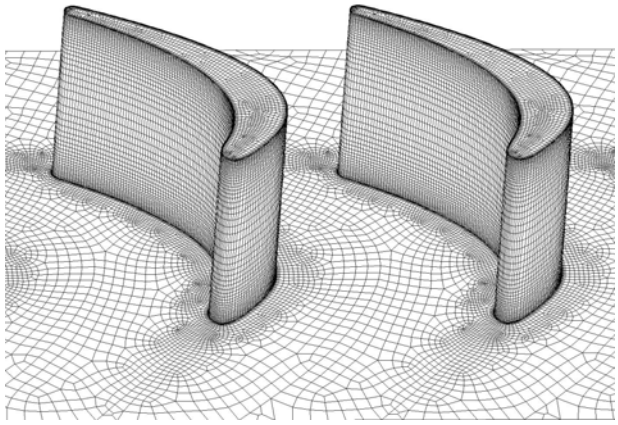

(a) Isometric view for the computational grid

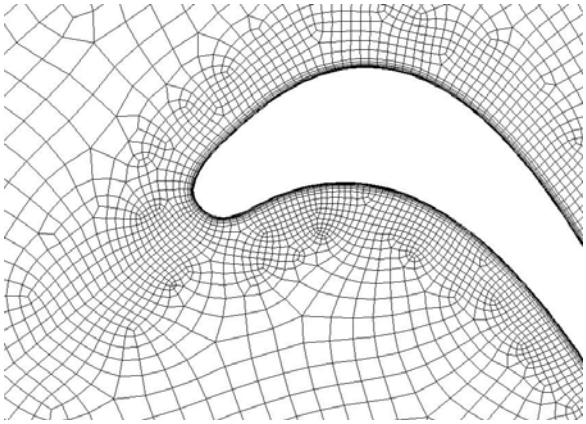

(b) The grid at the root

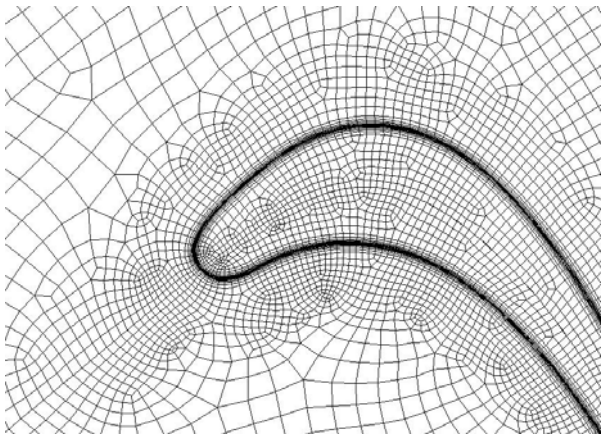

(c) Tip clearance grid

Figure 2: Computational grid

4. DATA REDUCTION

The loss mechanism is investigated by using the local total pressure coefficient which is defined as:

$$C_p = \frac{P_{t1} - P_t}{0.5\rho U_o^2} \qquad (9)$$

where P_{t1} is the total pressure at the inlet, P_t is the local total pressure and U_o is the exit velocity.

The total losses are estimated in terms of total pressure loss coefficient which is calculated using mass-averaging procedure. The total pressure loss coefficient C_{Pt} is calculated from:

$$C_{pt} = \frac{\overline{P_{t1}} - \overline{P_{t2}}}{0.5\rho \overline{U}_o^2} \qquad (10)$$

where $\overline{P_{t1}}$ is the mass-averaged total pressure at the inlet, $\overline{P_{t2}}$ is the mass-averaged total pressure at the outlet and $\overline{U}_o$ is the mass averaged exit velocity.

5. RESULTS

5.1 Flow Streamlines

Figure 3 shows flow streamlines through the cascade drawn in a plane crossing the blade at distance of 2.48 mm (2% of blade height) from the blade tip. The figure shows also the calculations for the case without tip clearance and the experimental measurements of El-Gendi [18] without tip clearance.

For the case without tip clearance, the flow streamlines show that passage vortex are generated from the blade pressure surface to the blade suction surface near the end-wall. The agreement between the numerical calculations and the experimental data are quite good. For the cases with tip clearances, the tip leakage flow passes from the pressure surface to the suction surface through the tip clearance. The passage vortex and the tip leakage flows have opposite directions which results in an interaction between them. The interaction between the tip leakage flow and passage vortex increases as the tip clearance gap decreases.

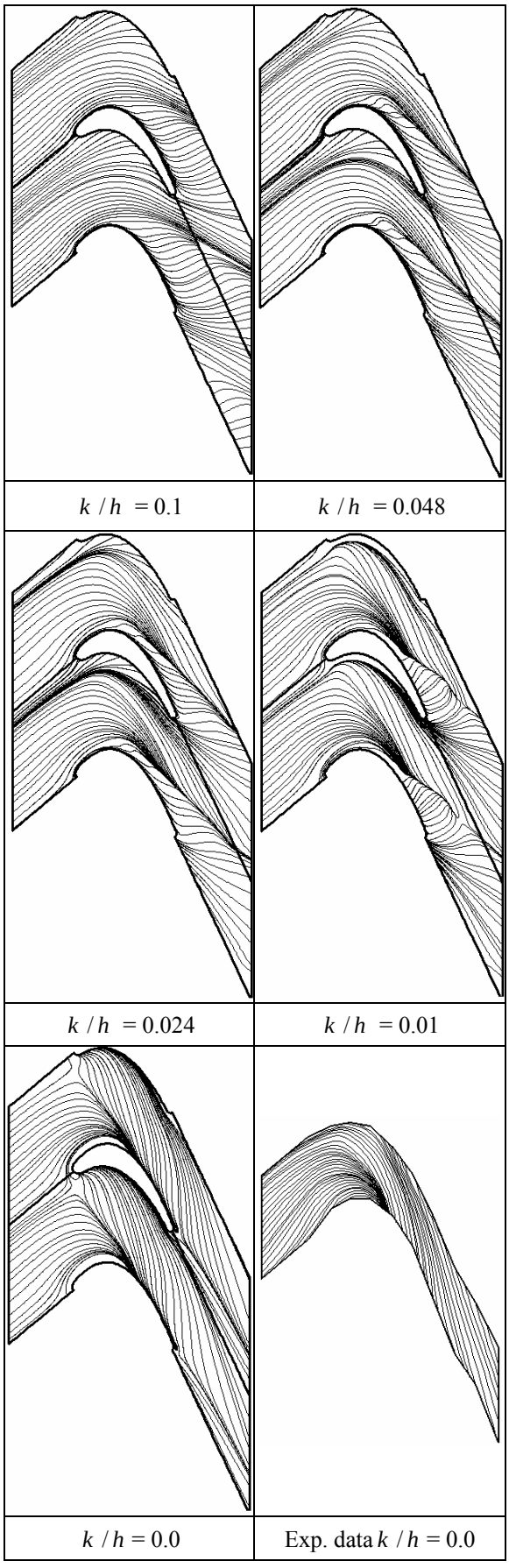

Figure 3: Streamlines at a distance 2.48 mm from the blade tip in the blade region

The flow streamlines in the tip clearance region are shown in figure 4 for the four values of tip clearance gaps considered in this study. The streamlines are drawn on the plane passing through the mid-distance of the tip clearance gap. The streamlines demonstrate the leakage flow from the pressure side to the suction side in the tip clearance gap. The figure indicates that by reducing the clearance gap, the flow structure becomes more complex due to interference between the tip leakage flow and the passage vortex.

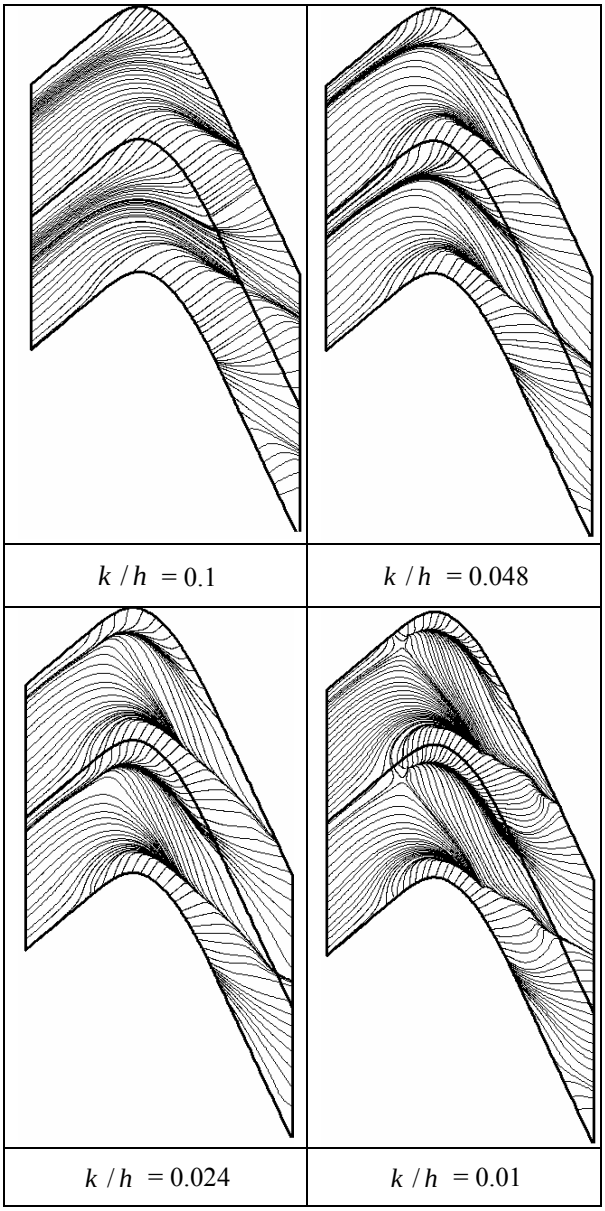

Figure 4: Streamlines at mid-clearance gap

5.2 Flow Vortices

In turbomachines, the losses are always calculated using mass-averaging procedure. In this procedure, the local loss coefficient is multiplied by the local mass flow rate. In this study, to illustrate the losses caused by the secondary flow and tip leakage flow, iso-surfaces are defined through the channel. These surfaces are defined at constant local total pressure coefficient. Then these surfaces are colored by using the local velocity magnitude as shown in figure 5. Therefore, this figure gives a direct indication about the loss distribution (from the location of the surfaces) and the contributions to the total losses (from the velocity magnitude).

For the cascade without tip leakage, the figure shows that passage vortex starts on the suction surface and propagates through the blade passage. The passage vortex from both end-walls is merged at the blade mid-span due to the low aspect ratio of the blade. The horseshoe vortex is also shown at the blade leading edge.

For the cases with tip clearance gaps another large vortex starts from the pressure surface to the suction surface due to the difference in pressures. This vortex propagates with the blade chord because the difference in pressure between the blade pressure side and the blade suction side increases along blade chord. The figure shows also that by increasing the tip clearance gap, the size of vortex increases.

Figures 6 and 7 show contours plots of the local total pressure coefficient at two locations downstream of the cascade. The planes are selected at distances of c_x equals to 1.1 and 1.32. The figures show that a large vortex caused by the tip leakage flow is generated in all cases of different tip clearance gaps. The size of the vortex decreases as the clearance gap decreases. This vortex can be distinguished in the selected planes downstream of the cascade. The comparison between the location of the vortex in the studied planes shows that the vortex moves from the blade pressure side to the blade suction side due to the difference in pressure between both sides of the blade. Passage vortex caused by the deflection through the cascade is also observed.

5.3 Total Losses

The total losses in turbine cascades are the sum of the profile loss, secondary flow loss and the tip leakage loss. In the present study, the total losses are calculated at various values of tip clearance gap. The losses are calculated also for the case without tip clearance gap. The differences between the losses in the cases with tip clearance gaps and that without tip clearance gap represent the tip leakage loss. Figure 8 shows the tip leakage losses for different values of tip clearance gaps. The figure indicates that the losses increase rapidly between the case with the minimum considered clearance gap and that without clearance gap. Then there is a linear relation between the gap distance and the losses.

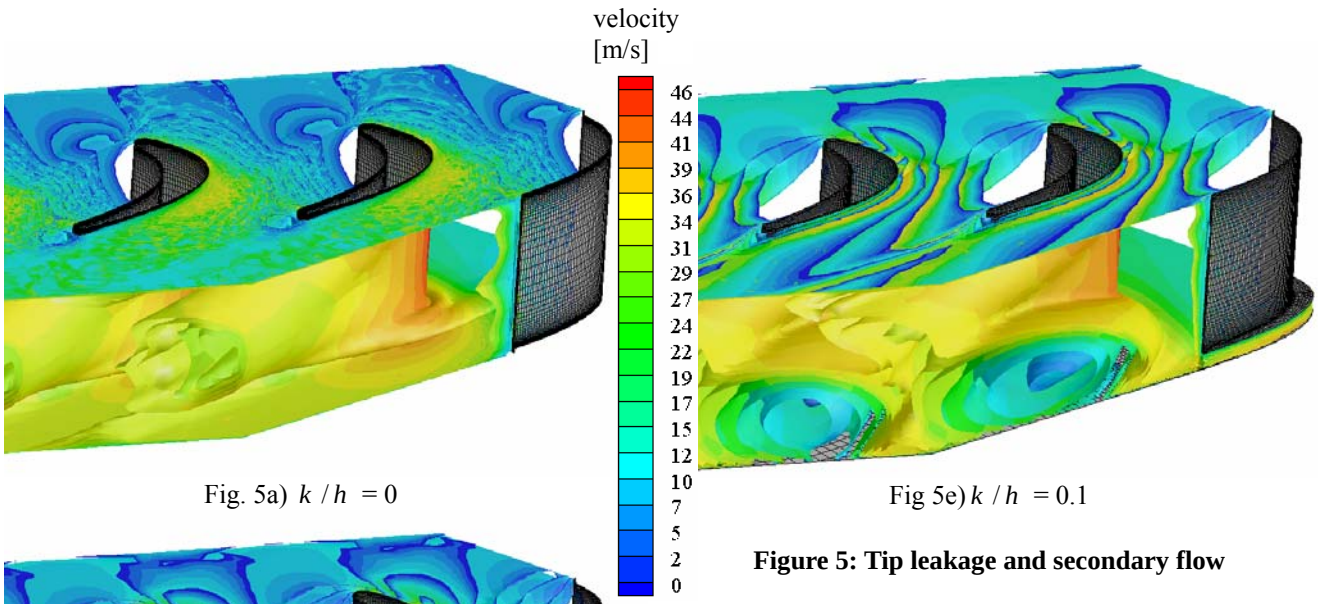

Fig. 5a) $k/h = 0$

Fig 5b) $k/h = 0.01$

Fig 5c) $k/h = 0.024$

Fig 5d) $k/h = 0.048$

Fig 5e) $k/h = 0.1$

Figure 5: Tip leakage and secondary flow

Matsunuma [19] reviewed various correlations of tip leakage loss C_{pTC} at different Reynolds numbers. For the value of Reynolds number used in this study, he found that the following correlation best fits the experimental data.

$$C_{pTC} = 0.5\left(\frac{k}{h}\right)\left(\frac{c}{s}\right)^2 C_L^2\left(\frac{\cos^2\beta_2}{\cos^2\beta_m}\right)\left(\frac{\mathrm{Re}}{2\times10^5}\right)^{-0.2}$$

The mean flow angle β_m is calculated from:

$$\beta_m = \tan^{-1}\left[\left(\tan\beta_2 - \tan\beta_1\right)/2\right]$$

The lift coefficient C_L is given by:

$$C_L = 2\left(s/c\right)\left(\tan\beta_2 + \tan\beta_1\right)\cos\beta_m$$

Reynolds number Re is calculated based on blade chord length and exit velocity.

This correlation supports the linear relation between the tip leakage loss and the tip clearance gap. Table 2 shows a comparison between the calculated losses in the present study and the losses estimated using the correlation. The comparison between the correlation and the numerical calculations shows that the error is about 9% when the clearance gap is 1% of the blade height. The error between the correlation and the CFD calculations increases as the clearance gap increases. The correlation is derived for typical values of clearance gap which is about 1% of the blade height. Using the correlation with large values of tip clearance gap introduces error in loss estimation using the correlation.

Table 2: Tip leakage loss

(k/h) [%]	Tip leakage loss C_{pTC} [–]	
	Calculation	Correlation
1.0	0.1035	0.095
2.4	0.1305	0.229
4.8	0.1995	0.46
10	0.3105	0.96

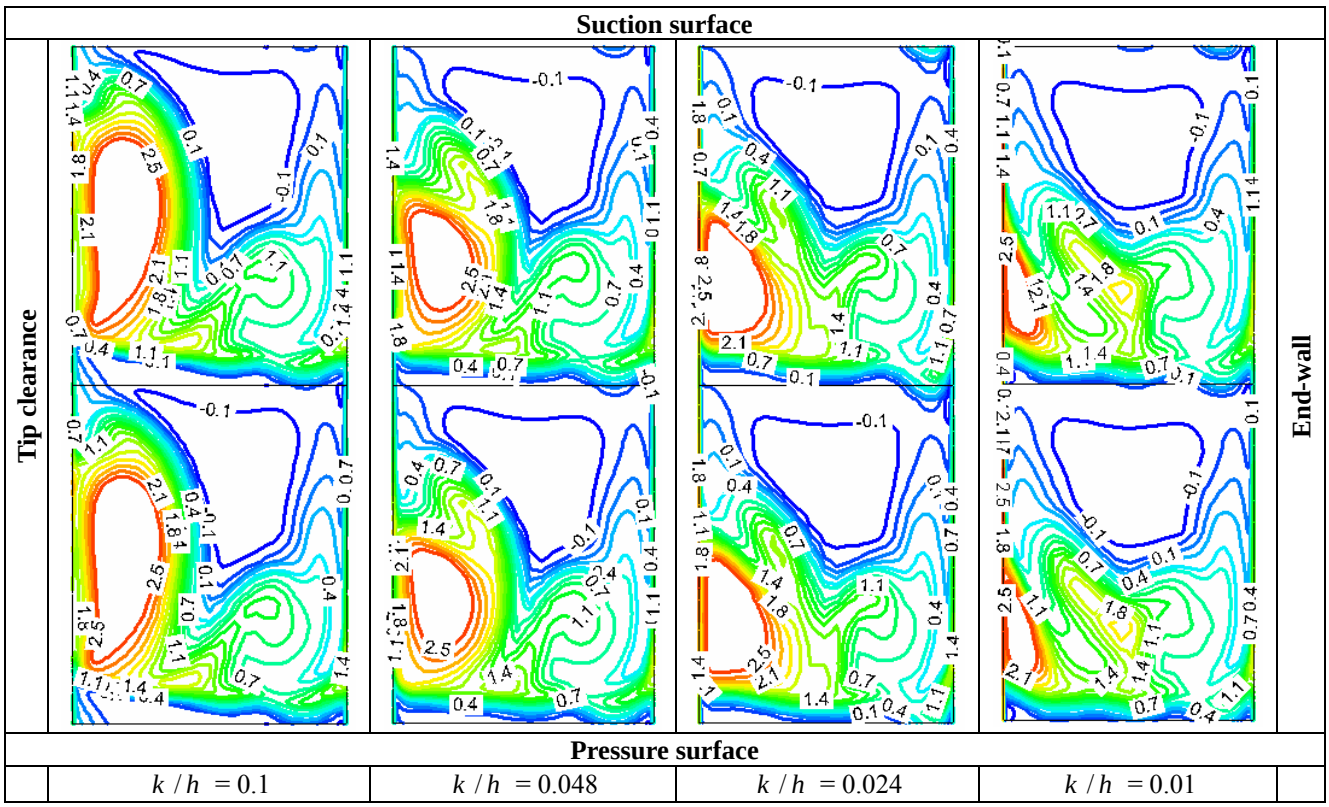

Figure 6: Contours of local total pressure coefficient downstream of the cascade, 1.1 axial chord

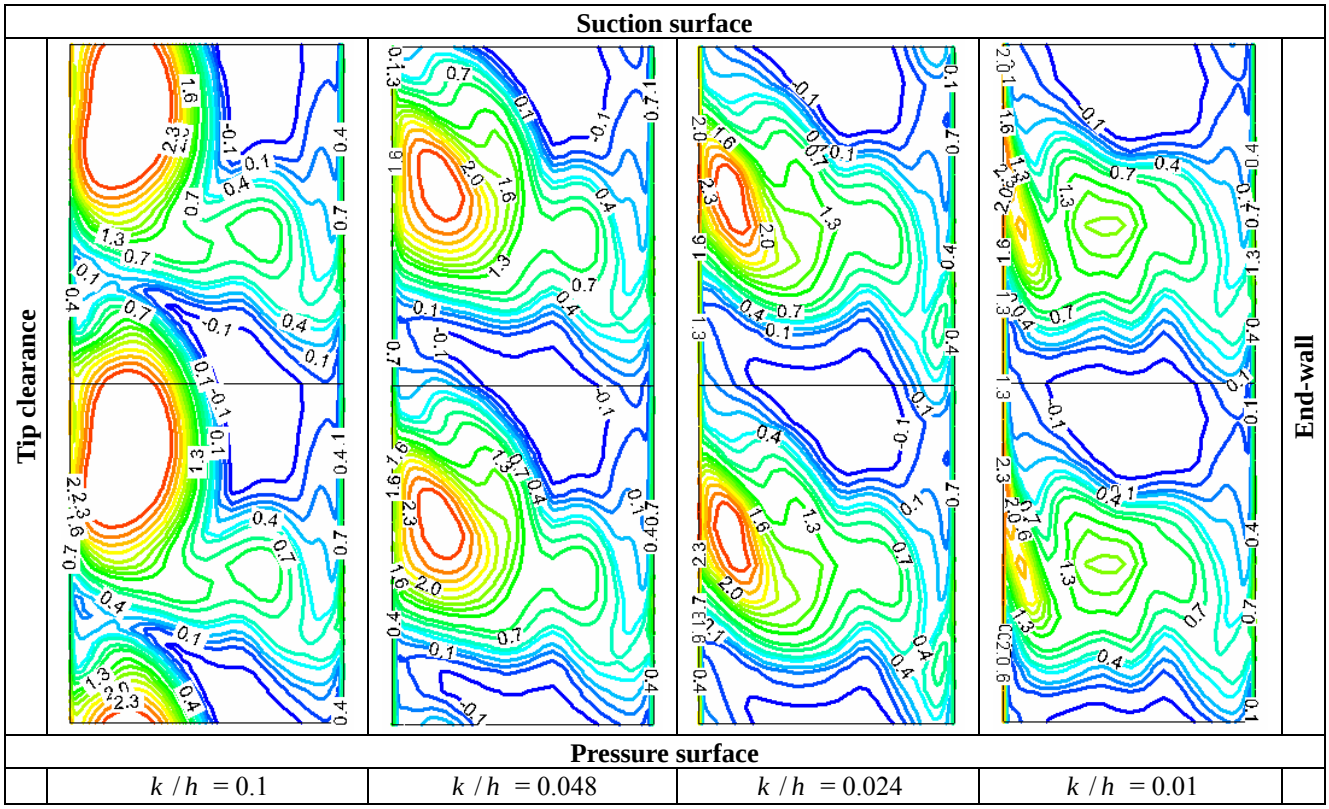

Figure 7: Contours of local total pressure coefficient downstream of the cascade, 1.32 axial chord

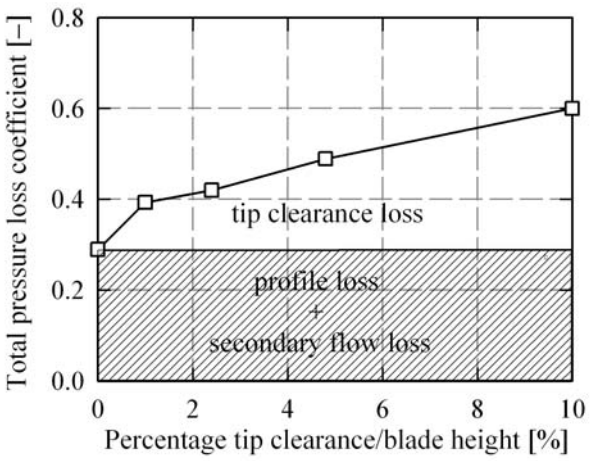

Figure 8: The losses through the cascade

6. CONCLUSIONS

Three-dimensional flow through a linear turbine cascade is investigated taking the effect of tip clearance into consideration. Different values of tip clearance gaps are studied. The loss mechanism caused by the tip leakage is examined. It is found through this study that the tip clearance generates a vortex which has an opposite direction to the passage vortex. The size of the vortex increases as the tip clearance gap increases. This vortex is the main cause of tip clearance loss. Tip clearance loss is estimated and agrees well with correlation prediction at typical values of tip clearances

REFERENCES

[1] El-Batsh, H., Numerical study of the flow field through a transonic linear turbine cascade at design and off-design conditions, Fourth International Engineering Conference, Mansoura-Sharm El-Sheikh, April 20-22, 2004.

[2] Sieverding, C. H., Recent progress in the understanding of basic aspects of secondary flows in turbine blade passages, Journal of Engineering for Gas Turbines and Power, Transactions of ASME, vol. 107, pp. 248-257, 1985.

[3] El-Batsh, H. and Bassily Hanna, M., Numerical and experimental prediction of secondary flow through a rectilinear cascade for different aspect ratios, Proceedings of the International Mechanical Engineering Conference, December 5-8, 2004, Kuwait.

[4] Denton, J. D., Loss mechanisms in turbomachinery, Journal of Turbomachinery, ASME Transactions, vol. 115, pp. 621–656, 1993.

[5] Moore, J. and Tilton, J.S., Tip leakage flow in a linear turbine cascade, Journal of Turbomachinery, ASME Transactions, vol. 110, pp. 18-26, 1988.

[6] Bindon, J. P., The measurement and formation of tip clearance loss, Journal of Turbomachinery, ASME Transactions, vol. 111, pp. 257-263, 1989.

[7] Yaras, M. I. and Sjolander, S. A., Effects of simulated rotation on tip leakage in a planar cascade of turbine blades: part I-tip gap flow, Journal of Turbomachinery, ASME Transactions, vol. 114, pp. 652–659, 1992.

[8] Yaras, M. I.; Sjolander, S. A., and Kind, R. J., Effects of simulated rotation on tip leakage in a planar cascade of turbine blades: part II-downstream flow field and blade loading, Journal of Turbomachinery, ASME Transactions, vol. 114, pp. 660–667, 1992.

[9] Willinger, R. and Haselbacher, H., Experimental and numerical investigation of the flow field in a linear turbine cascade including tip clearance effect, Transactions of the Institute of Fluid Flow Machinery, No. 104, 1998.

[10] Willinger. R. and Haselbacher. H., On the modeling of tip leakage flow in axial turbine blade rows, ASME paper No. 2000-GT-633, 2000.

[11] Krishnababu, S; Newton, P.; Dawes, B.; Lock, G. and Hodson, H., An experimental and numerical investigation of the tip leakage flow and heat transfer using a rotor tip gap model, 6th European Turbomachinery Conference, Fluid Dynamics and Thermodynamics, 7-11 March 2005, Lille, France.

[12] Langston, L. S.; Nice, M. L. and Hooper, R. M., Three-dimensional flow within a turbine cascade passage, Journal of Engineering for Power, Transactions of ASME, pp. 21-28, 1977.

[13] Sevilla, E., Experimental investigation of the systematic errors of pneumatic pressure probes induced by velocity gradients, Diploma Thesis, Institute of Thermal Turbomachines and Powerplants, Vienna University of Technology, 2002.

[14] Spalart, P. and Allmaras, S., A one-equation turbulence model for aerodynamic flows, Technical Report AIAA-92-0439, American Institute of Aeronautics and Astronautics, 1992.

[15] Hildebrandt, T. and Fottner, L., A Numerical study of the influence of grid refinement and turbulence modeling on the flow field inside a highly loaded turbine cascade, Journal of Turbomachinery, ASME Transactions, vol. 121, pp. 709-716, 1999.

[16] Casey, M. and Wintergerste, T., ERCOFTAC special interest group on quality and trust in industrial CFD, Best practice guidelines, 2000.

[17] Patankar, S., Numerical heat transfer and fluid flow, Taylor and Francis, 1980.

[18] El-Gendi, M., Effect of varying the aspect ratio on the secondary flow generated through a rectlinear accelerating blade cascade, M.Sc. Thesis, Faculty of Engineering, Minia University, Egypt, 2003.

[19] Matsunuma, T., Effect of Reynolds number and free stream turbulence on tip clearance flow, ASME paper No. GT 2005-68009, 2005.